2000-08

Noise equalization in Stokes parameter images obtained by use of variable-retardance polarimeters

Tyo, J. Scott

Noise equalization in Stokes parameter images obtained by use of variable-retardance polarimeters

J. Scott Tyo

Department of Electrical and Computer Engineering, U.S. Naval Postgraduate School, Monterey, California 93943

Received February 7, 2000

An imaging variable retardance polarimeter was developed and tested by Tyo and Turner [Proc. SPIE **3753,** 214 (1999)]. The signal-to-noise ratio (SNR) in the reconstructed polarization images obtained with this system varied for the four Stokes parameters. The difference in SNR is determined to be due to differences in the Euclidean lengths of the rows of the synthesis matrix used to reconstruct the Stokes parameters from the measured intensity data. I equalize (and minimize) the lengths of the rows of this matrix by minimizing the condition number of the synthesis matrix, thereby maximizing the relative importance of each of the polarimeter measurements. The performance of the optimized system is demonstrated with simulated data, and the SNR is shown to increase from a worst case of −3.1 dB for the original settings to a worst case of +5.0 dB for the optimized system. © 2000 Optical Society of America

OCIS codes: 260.5430, 230.5440.

Stokes vector (SV) imaging polarimeters have been developed for use in remote-sensing applications and have been demonstrated to improve target contrast,[1,2] reduce clutter,[1] aid in the defeat of intervening scatterers,[2,3] and provide orientation information about target features.[1,2] Polarimeters employ strategies motivated by ellipsometry to measure components of the Stokes vector at each pixel in a frame; however, there are significant differences between ellipsometric and imaging applications that place restrictions on the design of SV polarimeters. First, ellipsometers are often single-pixel (or few-pixel) devices, whereas SV imaging polarimeters are designed to make measurements at 10^4–10^6 locations simultaneously. Second, the signal-to-noise ratio (SNR) is often lower for SV imaging polarimeters than for ellipsometers because the illumination is usually passive for the former. Third, the temporal resolution needed for an operational SV polarimeter to image a moving target limits the dwell time for each measurement. These factors push the design of imaging polarimeters to require as few measurements as possible.

The Stokes vector is a widely accepted means to describe the polarimetric signature of incoherent radiation, and it is typically defined as $\mathbf{S} = [s_0\ s_1\ s_2\ s_3]^T$, where s_0–s_3 are the Stokes parameters. Polarimetric imaging systems have been developed to detect one-, two-, three-, and four-dimensional polarization information, and the number of measurements made must be greater than or equal to the dimensionality of the desired reconstruction. The Stokes vector is typically inferred from data measurements by solution of a system of linear equations for the unknown Stokes parameters in a least-squares sense.

Variable-retardance (VR) polarimetry uses two mechanically fixed, variable retarders and a fixed linear polarization analyzer to make a set of measurements from which the Stokes vector can be reconstructed.[4] VR polarimeters have no moving components, so they do not suffer from the image wander that is seen in more-traditional rotating compensator systems. The Mueller matrix for the VR system is $\mathbf{M} = \mathbf{LP}(\theta) \cdot \mathbf{VR}(\phi_2, \delta_2) \cdot \mathbf{VR}(\phi_1, \delta_1)$, where the three Mueller matrices on the right-hand side correspond to the individual optical components, θ is the angle of the polarizer, and ϕ_1 and ϕ_2 are the fast axis angles of the variable retarders, with retardances δ_1 and δ_2. Because square-law detectors sense intensity, only the s_0 component of the output Stokes vector can be measured. Taking the product of the first row of $\mathbf{M}$ with input Stokes vector $\mathbf{S}_{\text{in}}$ yields $s_{0,\text{out}}$:

$$I \propto s_{0,\text{out}} = M_{11}s_0 + M_{12}s_1 + M_{12}s_2 + M_{11}s_3 . \quad (1)$$

By choice of at least four combinations of $\{\delta_1, \delta_2\}$, a system of linear equations that relate measured intensity to the input Stokes vector is constructed. For the purposes of this Letter it is assumed that the number of measurements is equal to four. An analysis matrix $\mathbf{A}$ can be created with $A_{i,j} = M^{(i)}_{1,j}$, where $\mathbf{M}^{(i)}$ is the Mueller matrix of the ith configuration. When $\mathbf{A}$ is full rank, a synthesis matrix $\mathbf{B} = \mathbf{A}^{-1}$ can be calculated, permitting synthesis of the Stokes vector from the intensity measurements at each pixel.

An example of an imaging VR spectropolarimeter was presented in Ref. 4. That instrument had its linear polarization analyzer at 0° and the two retarders at $\phi_1 = 22.5°$ and $\phi_2 = 45°$. Measurements were made with $\{\delta_1, \delta_2\}$ set to {0°, 0°}, {0°, 90°}, {90°, 0°}, and {90°, 90°}. These settings were sufficient to permit unique reconstruction of the Stokes vector, but the apparent noise level was different in each of the four Stokes parameter images. This difference is demonstrated with simulated data in Fig. 1.

I constructed the 51-pixel × 51-pixel simulated images in Fig. 1 by setting the Stokes vector of the 25-pixel × 25-pixel central region to $\mathbf{S} = [\sqrt{3}\ 1\ 1\ 1]^T$. The outside region was set to $\mathbf{S} = \mathbf{0}$. This Stokes vector was operated on by the Mueller matrices corresponding to the system settings given above,[4] and the resultant s_0 values were calculated. Zero-mean white Gaussian noise with a variance of 0.10 was added to each of the four intensity images ($\sigma^2 = 0.10$, SNR of 15 dB). The Stokes parameter images were then constructed by use of the synthesis matrix on the noisy images.

0146-9592/00/161198-03$15.00/0

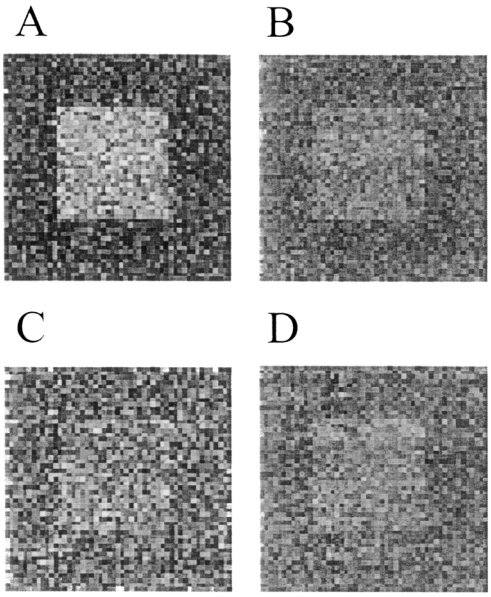

Fig. 1. Simulated noisy data from the VR parameter settings of Ref. 4. The actual image distribution has a Stokes vector of $[\sqrt{3}\ 1\ 1\ 1]^T$ in the central region and of $\mathbf{0}$ outside. The gray-scale axes are stretched to maximize the dynamic range. For A (s_0), the gray-scale range corresponds to reconstructed values from -2.93 to 4.13; for B, C, and D (s_1, s_2, and s_3), the range is from -5.70 to 5.53.

The nonuniform variance noted in Ref. 4 is evident in Fig. 1. The mean Stokes vector in the central region is $\langle \mathbf{S} \rangle = [1.76\ 0.97\ 0.99\ 1.03]^T$, where $\langle\ \rangle$ indicates a spatial average, so the average performance of the simulated system is accurate to within 3% but the variance is $\mathrm{var}(\mathbf{S}) = [0.62\ 0.44\ 2.07\ 0.60]^T$, where $[\mathrm{var}(\mathbf{S})]_i = \mathrm{var}(s_{i-1})$. The maximum SNR is 6.9 dB (s_0), and the minimum is -3.2 dB (s_2).

We can understand the differences in SNR among the reconstructed images (and the low SNR) by considering the properties of the analysis and synthesis matrices. If the noise variance is σ^2 in each of the four intensity images, the variance in the reconstructed images is

$$\mathrm{var}(s_i) = \sigma^2 \|\mathbf{B}_{i+1}\|_2{}^2, \tag{2}$$

where $\|\mathbf{B}_{i+1}\|_2$ is the Euclidean length of the $i + 1$st row of the synthesis matrix. For the synthesis matrix corresponding to Fig. 1 the lengths of the rows are $\{2.45, 2.08, 4.43, 2.45\}$, and the computed variances are within 5% of the predicted values. To equalize the noise in the reconstructed images one must also equalize the lengths of the rows of the inverse matrix (and minimize them to improve the SNR). In this study I obtained the equalization by minimizing the L_2 condition number of analysis matrix $\mathbf{A}$.

The L_p norm of matrix $\mathbf{A}$ is[5]

$$\|\mathbf{A}\|_p = \sup_{\mathbf{x}\in\mathcal{D}(\mathbf{A})} (\|\mathbf{A}\mathbf{x}\|_p / \|\mathbf{x}\|_p), \qquad (\|\mathbf{x}\|_p)^p = \sum_i x_i{}^p, \tag{3}$$

where $\mathcal{D}(\mathbf{A})$ is the domain of $\mathbf{A}$. The interested reader is referred to Ref. 5 for more information on various matrix and vector norms. Because the image variance is related to the Euclidean length of the rows of the synthesis matrix, the $\mathbf{L}_2$ matrix norm is chosen for optimization in this study. Other definitions of the SNR (in terms of other vector norms) would result in different optimizations.[6]

The condition number of a matrix is defined as $\kappa_p(\mathbf{A}) = \|\mathbf{A}\|_p \|\mathbf{A}^{-1}\|_p$, and one evaluates the L_2 condition number by taking the ratio of the largest to smallest singular value of the matrix as computed with the singular-value decomposition.[5] The higher the condition number, the less linearly independent are the columns of $\mathbf{A}$, so the rows of $\mathbf{A}^{-1}$ must have large L_2 lengths for inversion to be accomplished. Minimizing the condition number maximizes the relative importance of each of the four measurements, thereby increasing system stability and decreasing noise variance in the reconstructed images.

The optimization was accomplished with the sequential quadratic programming method in the Matlab (Ver. 5.3) Optimization Toolbox (Ver. 2). The angles of the variable retarders were fixed at 22.5° and 45°, and the four pairs of retardance values were varied to minimize $\kappa_2(\mathbf{A})$. The optimum settings obtained for VR polarimetry are nonunique, and one set of optimum retardances is given by $\{\delta_1, \delta_2\} = \{-3.59°, -16.3°\}$, $\{-61.1°, 134°\}$, $\{103°, 49.3°\}$, $\{107°, 156°\}$. The lengths of the rows of all numerically optimized synthesis matrices are $\{1, \sqrt{3}, \sqrt{3}, \sqrt{3}\}$ to five significant figures. For optimum configurations, the corresponding singular values are $\{1, 1/\sqrt{3}, 1/\sqrt{3}, 1/\sqrt{3}\}$. These results imply that the first measurement provides the most information about the polarization state and that each successive measurement provides the same amount of additional information. The sum of the squares of the singular values is 2, and this is equal to the number of orthogonal measurements that can be made with physical components; i.e., each polarization state has exactly one state that is orthogonal to it.

Simulated Stokes parameter images for the optimized configuration above are presented in Fig. 2, with $\langle \mathbf{S} \rangle = [1.74\ 0.99\ 1.01\ 0.98]^T$ and $\mathrm{var}(\mathbf{S}) = [0.10\ 0.31\ 0.29\ 0.30]^T$. The variance predicted by the lengths of the rows of $\mathbf{B}$ is $\mathrm{var}(\mathbf{S}) = [0.10\ 0.30\ 0.30\ 0.30]^T$. The maximum SNR has been increased to 15 dB for s_0, and the SNR's for s_1–s_3 have been nearly equalized to 5.1 dB.

There is an elegant graphical construct first proposed in Ref. 6 that helps to clarify the results described above. The two retarders and the linear polarizer together form an elliptical diattenuator. The intensity of one elliptically polarized state is unattenuated on transmission; the intensity of the orthogonal polarization state is completely extinguished. The unattenuated state has a unique Stokes vector that is termed here the principal direction of the system. As the system parameters are varied, the principal direction traces out a trajectory on the Poincaré sphere. The optimization procedure is equivalent to choosing a best set of four locations from that trajectory. Ambirajan and Look[6] hypothesized that an optimal configuration inscribes a regular tetrahedron inside the Poincaré sphere. Although

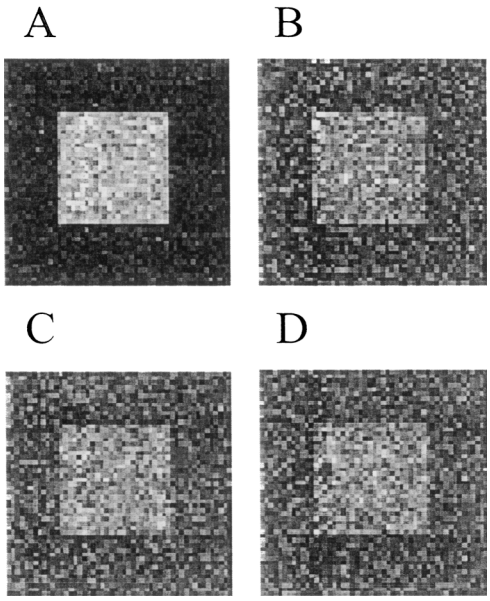

Fig. 2. Simulated data for the optimized settings given in this study. Actual image distributions are the same as in Fig. 1. The gray-scale ranges maximize dynamic range and are different from those in Fig. 1. The gray-scale range corresponds to reconstructed values from −0.96 to 2.79. For B, C, and D (s_1, s_2, and s_3) the range is from −2.04 to 2.98. The optimization is not restricted to this particular Stokes vector, as the system condition is independent of the input.

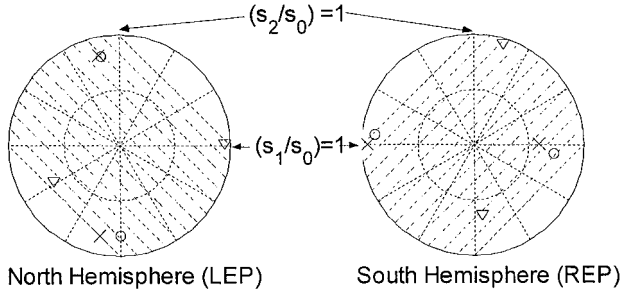

Fig. 3. Regions accessible by the VR polarimeter with $\phi_1 = 22.5°$ and $\phi_2 = 45°$. These are polar projections with left- and right-elliptically polarized (LEP and REP) states in the north and south hemispheres, respectively. The straight lines actually form coaxial circles on the Poincaré sphere. The common axis bisects the angle between the s_1 and s_2 axes. The points form inscribed regular tetrahedrons and are optimal configurations. Crosses, {158°, 50.6°}, {127°, −178°}, {47.0°, −16.9°}, and {0.659°, 126°}. Circles, {160°, 50.1°}, {−10.1°, 144°}, {89.8°, −144°}, and {57.4°, −12.9°}. Triangles, values in the text.

they were unable to achieve the optimization, the results presented here and in Ref. 7 verify the hypothesis.

For rotating compensator systems, there is only one degree of freedom (angle of the retarder), so the trajectory forms a curve on the Poincaré sphere. There are exactly two ways to inscribe a regular tetrahedron whose corners lie upon the trajectory when the compensator has a retardance of 0.37λ.[7] The VR system has two degrees of freedom (retardance values), so the trajectory maps out a surface, as shown in Fig. 3. The hatched areas indicate the parts of the Poincaré sphere that can be reached by the polarimeter, and three sets of optimal retardance are indicated. There is a continuum of optimal configurations that fit inside this region. For the optimization presented here, $\phi_1 = 22.5°$ and $\phi_2 = 45°$ because of the relation to the research presented in Ref. 4. These are not the only angles that will produce at least one optimum, and not all angle pairs are guaranteed to produce even one optimum. For example, the best configuration possible with $\phi_1 = 45°$ and $\phi_2 = 22.5°$ is suboptimal ($\kappa_2 = 2.48$). For VR systems with $\phi_2 = 45°$, optimal configurations exist for $-27° < \phi_1 < 27°$.

The minimization procedure performed here is equivalent to that performed by Sabatke *et al.*,[7] for which the total noise power (summed over all Stokes parameter images) was minimized for rotating compensator polarimeters. Ambirajan and Look[6] considered the L_1 and L_∞ condition numbers and the magnitude of the determinant in optimizing rotating quarter-wave-plate systems. Tyo[8] examined the correlation between the individual measurements of a rotating analyzer system to determine the conditions for optimum information reconstruction. These analyses produce equivalent results and are fundamentally related.

The methods described here can be extended to any dimensionality of polarimeter with any number of measurements used to select an optimum configuration. There is no evidence that indicates that one optimal configuration is preferable to another, but experimental considerations, background polarization biases, and the effect of instrumental error may provide a reason to select a particular optimal solution.

The author's e-mail address is tyo@ieee.org.

References

1. L J. Cheng, J. C. Mahoney, and G. Reyes, Proc. SPIE **2237,** 251 (1994).
2. J. S. Tyo, M. P. Rowe, E. N. Pugh, and N. Engheta, Appl. Opt. **35,** 1855 (1996).
3. M. P. Silverman and W. Strange, Opt. Commun. **144,** 7 (1997).
4. J. S. Tyo and T. S. Turner, Jr., Proc. SPIE **3753,** 214 (1999).
5. G. H. Golub and C. F. van Loan, *Matrix Computations* (Johns Hopkins U. Press, Baltimore, Md., 1983), Chap. 2, pp. 11–29.
6. A. Ambirajan and D. C. Look, Jr., Opt. Eng. **34,** 1651, 1656 (1995).
7. D. S. Sabatke, M. R. Descour, E. Dereniak, W. C. Sweatt, S. A. Kemme, and G. S. Phipps, Opt. Lett. **25,** 802 (2000).
8. J. S. Tyo, J. Opt. Soc. Am. A **15,** 359 (1998).